Coupled Hydro – Aero – Elastic Analysis of a Multi – Purpose Floating Structure for Offshore Wind and Wave Energy Sources Exploitation

Thomas P., Mazarakos, *Laboratory for Floating Structures and Mooring Systems, School of Naval Architecture and Marine Engineering,* tmazarakos@naval.ntua.gr

Dimitrios N., Konispoliatis, *Laboratory for Floating Structures and Mooring Systems, School of Naval Architecture and Marine Engineering,* dkonisp@naval.ntua.gr

Dimitris I., Manolas, *Aerodynamic Laboratory, School of Mechanical Engineering National Technical University of Athens,* manolasd@fluid.mech.ntua.gr

Spyros A., Mavrakos, *Laboratory for Floating Structures and Mooring Systems, School of Naval Architecture and Marine Engineering,* mavrakos@naval.ntua.gr

Spyros G., Voutsinas, *Aerodynamic Laboratory, School of Mechanical Engineering National Technical University of Athens,* spyros@fluid.mech.ntua.gr

ABSTRACT

A coupled hydro–aero–elastic analysis of a multi–purpose floating structure suitable for offshore wind and wave energy sources exploitation is presented. The floating structure encompasses an array of hydrodynamically interacting Oscillating Water Column (OWC) devices consisting of concentric vertical cylinders, which are moored through tensioned tethers as a Tension Leg Platform (TLP) supporting a 5 MW W/T. The solutions of the diffraction and the pressure– and motion– dependent radiation problems around the floating structure and the aerodynamics of the Wind Turbine (W/T) are properly combined in the frequency and time domain. Results are compared at the level of RAOs and consistent results are obtained.

Keywords: *Multi purpose floating structure, Oscillating water column device, Wind turbine*

1. INTRODUCTION

In the last years considerable efforts and advances have been made worldwide in developing renewable energy devices. Among the numerous concepts proposed for wave energy conversion one of the most promising is the multi bodied floating structure based on the oscillating water column principle. Such type of devices have been reported in connection with the wave energy extraction (Konispoliatis & Mavrakos, 2013a) or in composing semi–submersible platforms for renewable electricity generation from the combined wind and wave action (Aubault et al., 2011; Mavrakos et al., 2011).

In the present contribution we consider a system of three identical OWC devices which

are placed at the corners of a triangular floater and can oscillate about their mean equilibrium position moving as a unit. The geometric configuration of each device consists of an exterior partially immersed toroidal oscillating chamber of finite volume supplemented by a concentric interior piston– like truncated cylinder. The wave action causes the captured water column to oscillate in the annular chamber, compressing and decompressing the air above the inner water surface. As a result, there is an air flow moving forwards and backwards through a turbine coupled to an electric generator. In the centre of the platform a solid cylindrical body is arranged in order to support the W/T (Figure 1).

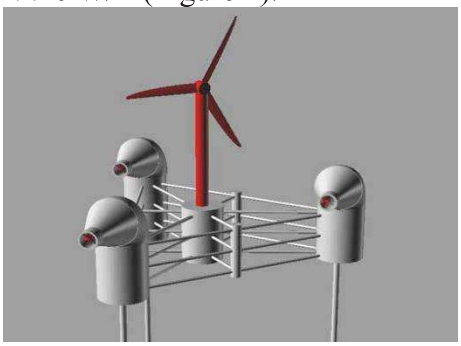

Figure 1: Multi-purpose floating structure with three OWC devices and a W/T

The latter is a typical 5MW horizontal axis turbine which is a variable- speed variable-pitch controlled WT. Detailed data are given in Jonkman et al. 2009. The tower of the WT is cantilevered at an elevation of 10m above the sea water level (SWL) to the top of the main column of the floating platform.

2. FORMULATION OF THE PROBLEM

2.1 Calculation of the velocity potential function

We consider that the group of three OWCs is excited by a plane periodic wave of amplitude $H/2$, frequency ω and wave number k propagating in water of finite water depth d. The distance between each device is L. The outer and inner radii of each device's chamber q, q=1, 2, 3, are denoted by α_q, b_q, respectively, whereas the distance between the bottom of the q device and the sea bed is denoted by h_q. The radius of the interior concentric cylindrical body in each device q, is denoted by $b_{1,q}$ and the distance between its bottom and the sea bed is $h_{1,q}$. The radius of the central cylindrical body that supports the WT is c and the distance between its bottom and the sea bed is h_c (Fig2 & Fig3). Small amplitude waves, inviscid, incompressible and irrotational flow are assumed, so that linear potential theory can be employed. A global Cartiesian co–ordinate system O–XYZ with origin on the sea bed and its vertical axis OZ directed positive upwards and coinciding with the vertical axis of symmetry of the central body is used. Moreover, three local cylindrical co-ordinate systems (r_q,θ_q,z_q), q = 1, 2, 3 are defined with origins on the sea bottom and their vertical axes pointing upwards and coinciding with the vertical axis of symmetry of the q device.

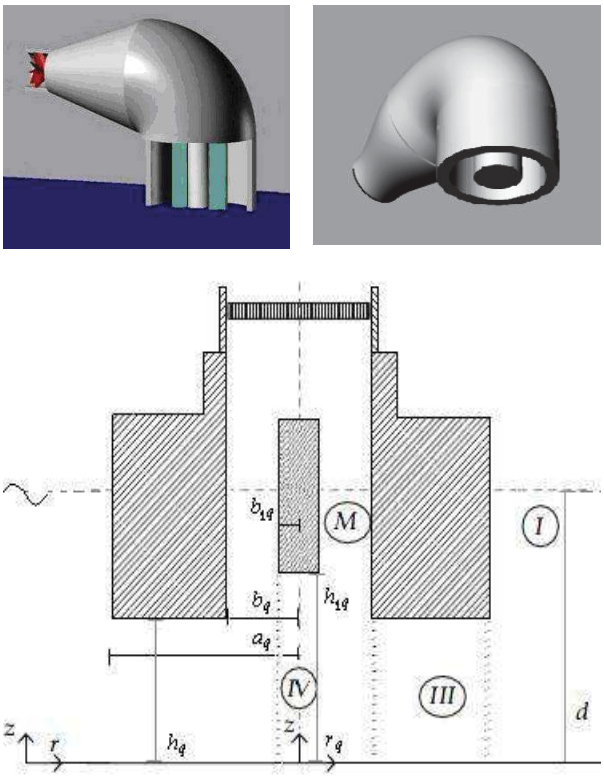

Figure 2: Definition sketch of the q OWC device of the array

The fluid flow around the q = 1, 2, 3, 4 device/body (three OWCs & one solid body) can be described by the potential function:

$$\Phi^q\left(r_q,\theta_q,z;t\right)=\mathrm{Re}\left\{\phi^q\left(r_q,\theta_q,z\right)\cdot e^{-i\omega t}\right\} \qquad (1)$$

Following Falnes (2002) the spatial function ϕ^q can be decomposed, on the basis of linear modelling, as:

$$\varphi^q=\varphi_0^q+\varphi_7^q+\sum_{p=1}^{4}\sum_{j=1}^{6}\dot{x}_{j0}^p\cdot\varphi_j^{qp}+\sum_{i=1}^{3}p_{in0}^i\cdot\varphi_P^{qi} \qquad (2)$$

Here, ϕ_0^q is the velocity potential of the undisturbed incident harmonic wave (Mavrakos & Koumoutsakos, 1987); ϕ_7^q is the scattered potential around the q device/body, when it is considered fixed in waves with the duct open to the atmosphere, so that the pressure in the chamber is equal to the atmospheric one (for the OWCs); ϕ_j^{qp} is the motion–dependent radiation potential around the device/body q resulting from the forced oscillation of the p–th device/body, p=1,2,3,4, moving with unit velocity amplitude, $\dot{x}_j^p=\mathrm{Re}\left\{\dot{x}_{j0}^p\cdot e^{-i\omega t}\right\}$; ϕ_P^{qi} is the pressure–dependent radiation potential around the q–th device/body when it is considered fixed in the wave field and open to the atmosphere (for the OWCs), due to unit time harmonic oscillating pressure head, $P_{in}^i=\mathrm{Re}\left\{p_{in0}^i\cdot e^{-i\omega t}\right\}$, in the chamber of the i=1,2,3 device which is considered fixed in otherwise calm water.

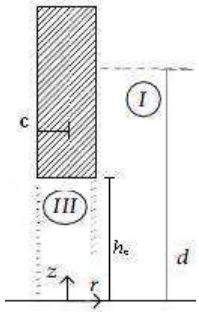

Figure 3: Definition sketch of the central cylindrical body basing the W/T

The diffraction, i.e. $\phi_D^q=\phi_0^q+\phi_7^q$, q=1,2,3,4, the motion– dependent radiation potentials around the isolated q device/body and pressure–dependent radiation potential around the isolated q device, when it is considered alone in the field, are expressed in its own cylindrical co–ordinate system $\left(r_q,\theta_q,z\right)$ as follows:

$$\phi_D^q(r_q,\theta_q,z)=-i\omega\frac{H}{2}\sum_{m=-\infty}^{\infty}i^m\Psi_{D,m}^q(r_q,z)\cdot e^{im\theta_q} \qquad (3)$$

$$\phi_j^{qq}(r_q,\theta_q,z)=-i\omega\sum_{m=-\infty}^{\infty}\Psi_{j,m}^{qq}(r_q,z)\cdot e^{im\theta_q} \qquad (4)$$

$$\phi_P^{qq}(r_q,\theta_q,z)=\frac{1}{i\omega\rho}\sum_{m=-\infty}^{\infty}\Psi_{P,m}^{qq}(r_q,z)\cdot e^{im\theta_q} \qquad (5)$$

Here ρ is the water density.

The potentials ϕ_j^l ($l\equiv q,\ qp$; j=D, 1, …, 6, P; p, q = 1,2,3,4; i=1,2,3) are solutions of Laplace's equation in the entire fluid domain and satisfy the following boundary conditions:

$$\omega^2\phi_j^l-g\frac{\partial\phi_j^l}{\partial z}=\begin{cases}0 & \text{for } r_q\ge a_q;\text{ or } r_q\ge c\\ & l\equiv q,\ j=D;\quad\text{or}\\ & l\equiv qp,\ j=1,2,\ldots,6,P\\ 0 & \text{for } b_{1,q}\le r_q\le b_q;\\ & l\equiv q,\ j=D;\quad\text{or}\\ & l\equiv qp,\ j=1,2,\ldots,6\\ -\delta_{q,i}\dfrac{i\omega}{\rho} & \text{for } b_{1,q}\le r_q\le b_q;\\ & l\equiv qi;\ j=P\end{cases} \qquad (6)$$

on the outer and inner free sea surface $\left(z=d\right)$, and the zero normal velocity on the sea bed $\left(z=0\right)$. Moreover, the potentials have to fulfil kinematic conditions on the mean device/body's wetted surface. Finally, a radiation condition must be imposed which states that propagating disturbances must be outgoing.

The unknown potential functions $\Psi_{j,m}^{k,l}$, k=I, III, M, IV, see Eq3 – Eq5, can be established in each fluid region surrounding the q–th device/body (see Figs. 2 and 3) using the method of matched axisymmetric eigenfunction expansions.

Next, the potentials, ϕ_j^{qp}, ϕ_P^{qi}, (j=1, …, 6) around anybody q of the multi – body configuration due to oscillation of body p,

p=1,2,3,4, in otherwise still water (motion – dependent radiation potential) or due to inner time harmonic oscillating pressure head in the air chamber of the device i, i=1,2,3, (pressure – dependent radiation potential), can be expressed in the q–th body's cylindrical coordinate system, as:

$$\phi_j^{qp}(r_q,\theta_q,z) = -i\omega \sum_{m=-\infty}^{\infty} \Psi_{j,m}^{qp}(r_q,z)\cdot e^{im\theta_q} \tag{7}$$

$$\phi_p^{qi}(r_q,\theta_q,z) = \frac{1}{i\omega\rho} \sum_{m=-\infty}^{\infty} \Psi_{p,m}^{qi}(r_q,z)\cdot e^{im\theta_q} \tag{8}$$

In order to express the potentials, ϕ_j^{qp}, ϕ_p^{qi} in the form of Eq7 and Eq8, use is made of the multiple scattering approach (Twersky, 1952; Okhusu, 1974). This method has been further elaborated to solve the diffraction and the motion – dependent radiation problems around arbitrarily shaped, floating or / and submerged vertical axisymmetric bodies by Mavrakos & Koumoutsakos (1987) and Mavrakos (1991) and for the diffraction and the pressure–dependent radiation problems for an interacting array of OWC's devices by Konispoliatis & Mavrakos (2013b); thus, it will be no further elaborated here.

2.2 Volume flow

The time dependent volume flow produced by the oscillating internal water surface in q OWC device, q = 1, 2, 3, is denoted by $Q^q(r_q,\theta_q,z;t) = \mathrm{Re}\left[q^q(r_q,\theta_q,z)\cdot e^{-i\omega t}\right]$, where:

$$q^q = \iint_{S_i^q} u_z\, dS_i^q = \iint_{S_i^q} \frac{\partial \phi^q}{\partial z} r_q\, dr_q\, d\theta_q \tag{9}$$

Here u_z denotes the vertical velocity of the water surface, and S_i^q the inner water surface in the q device, q=1, 2, 3.

Assuming that the Wells turbine is placed in a duct between the q device's chamber and the outer atmosphere and that it is characterized by a pneumatic admittance Λ^q, then the total volume flow is equal to (Evans & Porter; 1996, Falnes; 2002):

$$Q^q(t) = \Lambda^q \cdot P_{in}^q(t) \tag{10}$$

Assuming isentropy so that variations of air density and pressure are proportional to each other with $c_{air}^2 = dp_{in}^q / d\rho_{air}$, c_{air} being the sound velocity in air, the pneumatic complex admittance Λ^q is equal to (Martins–Rivas & Mei, 2010):

$$\Lambda^q = \frac{KD}{\rho_{air} N} + (-i\omega)\frac{V_0^q}{c_{air}^2 \rho_{air}} \tag{11}$$

Where K is constant for a given turbine geometry (independent of turbine size or rotational speed), D is turbine rotor diameter, N is the rotational speed (radians per unit time), ρ_{air} is the atmospheric density and V_0^q the q device's air chamber volume.

Decomposing the total volume flow, q^q, of the q–th device, same as for the velocity potential; see Eq2, into three terms associated with the diffraction, q_D^q, and the motion– and pressure–dependent radiation problems, q_R^q, q_P^q, respectively, we can obtained:

$$q^q = q_D^q + q_R^q + \sum_{i=1}^{3} p_{in0}^i \cdot q_P^{qi} \tag{12}$$

Here:

$$q_R^q = \sum_{p=1}^{4}\sum_{j=1}^{6} \dot{x}_{j0}^p \cdot q_{3,j}^p - \dot{x}_{30}^p \cdot S_i^p \tag{13}$$

Where S_i^p is the inner water surface in the p device, p=1, 2, 3.

The pneumatic admittance Λ^q for the OWCs, for the presented results, was considered as a real and positive number equal to the optimum coefficient Λ_{opt} of the same restrained OWC device but in isolation condition as in Evans and Porter (1996) work.

2.3 Hydrodynamic forces

The various forces on the q device/body can be calculated from the pressure distribution given by the linearised Bernoulli's equation:

$$P(r_q,\theta_q,z;t) = -\rho\frac{\partial\Phi^q}{\partial t} = i\omega\rho\phi^q\cdot e^{-i\omega t} \qquad (14)$$

Where ϕ^q is the q devices' velocity potential in each fluid domain *I*, *III*, *M* and *IV* (see Figs. 2 and 3). The horizontal and vertical exciting forces and moments acting on an array of OWC devices have been presented in Konispoliatis & Mavrakos (2013b).

The hydrodynamic reaction forces and moments F_{ij}^{qp} acting on the device/body q, q=1,2,3,4, in the i–th direction due to the oscillation of device/body p, p=1,2,3,4, in the j–th direction, can be calculated by the Eq14 and the complex form f_{ij}^{qp} may be written in the form (Newman, 1977):

$$f_{ij}^{qp} = \omega^2(a_{ij}^{qp} + {}^{i}\!/\!_{\omega}\, b_{ij}^{qp})x_{j0}^{p} \qquad (15)$$

Here, a_{ij}^{qp}, b_{ij}^{qp}, are the well–known added mass and damping coefficients.

In the same way, the hydrodynamic pressure forces and moments f_i^{ql} acting on the device/body q in the i–th direction due to oscillating pressure head in the l=1,2,3 device can be written in the form:

$$f_i^{ql} = \left(-e_i^{ql} + id_i^{ql}\right)\cdot p_{in0}^{l} \qquad (16)$$

Here e_i^{ql}, d_i^{ql} are the pressure damping coefficients.

The total hydrodynamic forces on the entire multi–body configuration can be calculated by properly superposing the corresponding forces on each device with respect to the reference point of motion, *G*, of the entire structure. (for details see Mavrakos, 1991).

2.4 Mooring system

The floating structure is moored with a TLP mooring system of three tendons spread symmetrically about the platform Z-axis. The fairleads are located at the base of the offset columns, at a depth of 20.0m below the sea water level. The anchors (fixed to the inertia frame) are located at a water depth of 200m below the sea water level. Each of the 3 tendons has an unstretched length of 180m, a diameter of 0.130m, an equivalent mass per unit length of 104kg/m and a submerged weight per unit length equal to 888.6N/m. The pretension of each tendon is 10800 kN. The mooring line stiffness k_{xx} and k_{zz} of each tendon is 60KN/m and 14700KN/m, respectively.

2.5 Aerodynamic loading

In the frequency domain formulation, the contribution of the W/T is projected on the degrees of freedom of the floater motion. This is carried out in the context of Hamiltonian dynamics with gravity and aerodynamics being the external forcing. The aerodynamic loading is defined from the Blade Element Momentum theory. After a linearization procedure, additional mass, damping and stiffness matrices are defined which contribute the W/T aerodynamic, inertial-gyroscopic and gravitational loading (Papadakis et al. 2014).

2.6 The time domain problem

The time domain simulations are carried out using the advanced full model hydroGAST developed at NTUA (Riziotis et al., 1997, 2004, Manolas et al. 2012). hydroGAST is a multi-body FEM dynamic model of the complete system. The aerodynamic loading is based on BEM modeling, the hydrodynamic loading is based on linear theory, and the mooring tendons as co-rotating non-linear truss elements. The specific model has been verified within the OC4 IEA project (Popko et al., 2012, Robertson et al., 2014a).

3. RESPONSE AMPLITUDE OPERETORS (RAO'S)

The investigation of the dynamic equilibrium of the forces acting on the freely floating array of OWC devices/body without the W/T leads to the following well – know system of differential equations of motions, in the frequency domain, i.e.:

$$\sum_{j=1}^{6}\left[-\omega^2(M_{i,j}+A_{i,j}+\frac{i}{\omega}B_{i,j})+C_{i,j}\right]\cdot x_{j0}-F_{P,i}=F_i \qquad (17)$$

for i=1,…,6.

where $M_{i,j}$ and $C_{i,j}$ are elements of the (6x6) mass and stiffness matrices of the entire configuration; $A_{i,j}, B_{i,j}$, are the hydrodynamic masses and potential damping of the entire configuration; F_i are the exciting forces acting on the multi–body system at the i–th direction; $F_{P,i}$ are the pressure hydrodynamic forces acting on the multi–body system at the i–th direction; x_{j0} is the motion displacement of the entire OWC system at the j–th direction with respect to a global co – ordinate system G.

By inserting the TLP mooring system and the W/T characteristics in the multi – body system, Eq17 can be reduced to the following form (Mazarakos et al. 2014a), describing the couple hydro – aeroelastic problem of the investigated moored multi-purpose floating structure in the frequency domain:

$$\sum_{j=1}^{6}\begin{bmatrix}-\omega^2(M_{i,j}+A_{i,j}+M^{WT}\\+\frac{i}{\omega}B_{i,j}+\frac{i}{\omega}B^{WT}_{i,j})\\+C_{i,j}+C^{WT}_{i,j}+C_{mooring}\end{bmatrix}\cdot x_{j0}= \qquad (18)$$
$$=F_i+F_{P,i}$$

where M^{WT}, B^{WT} and C^{WT}, are the mass, damping and stiffness which contribute the W/T aerodynamic, inertial-gyroscopic and gravitational loading respectively, while $C_{mooring}$ is the mooring lines stiffness matrix.

The RAO's can be estimated from time series data from the following equation:

$$RAO(\omega)=\frac{|P_{xy}(\omega)|}{P_{xx}(\omega)} \qquad (19)$$

where P_{xx} is the auto power spectral density and P_{xy} is the cross spectral density. P_{xx}, P_{xy} are calculated using Welch's method with a sufficient number of data split and 50% overlap between the split data parts. x refers to the input (wave elevation) and y to the output (each motion). The simulations lasted 3600sec - the first 600sec are excluded – assuming a uniform wind speed and white noise waves of 1m significant wave height.

4. NUMERICAL MODELING

4.1 Eigen values

In Table 1 the first 12 eigenvalues of the coupled system are presented, as provided by hydroGAST. In the flexible case, the flexibility of the W/T's members (tower, shaft, blades) is considered, while in the rigid case the members are stiff. The rigid case corresponds to the frequency domain analysis as well, because

only the 6 rigid modes of the floater are considered.

The main differences, between the two cases, are: the reduction of the roll/pitch eigenvalues from 0.3 Hz to 0.25 Hz and the presence of the tower fore-aft and side-to-side frequencies at ~0.85 Hz. Flexibility is important in the TLP case due to the strong coupling between the roll/pitch motion and the side-to-side/fore-aft bending moments of the tower. The modes of the blades and the shaft are not coupled with the motions of the floater, so they are not expected to appear in the RAOs.

Table 1: Coupled system eigen values [Hz]

Mode description	**flexible**	**rigid**
Platform Surge	0.026	0.026
Platform Sway	0.026	0.026
Platform Yaw	0.028	0.028
Platform Roll	**0.244**	**0.301**
Platform Pitch	**0.245**	**0.301**
Platform Heave	0.569	0.569
1st Drivetrain Torsion	0.585	-
1st Blade Flapwise Yaw	0.634	-
1st Blade Flapwise Pitch	0.653	-
1st Blade Collective Flap	0.702	-
1st Tower Fore-Aft	**0.854**	-
1st Tower Side-Side	**0.861**	-

4.2 RAO's comparison

Frequency and time domain methods consistently predict similar RAOs, in the case of a TLP floating W/T (Mazarakos et al. 2014b). In the present paper, RAOs for the TLP floating W/T with 3 OWC devices predicted by the frequency domain (fd) and the time domain (td) method are compared. Two inflow conditions are modelled; the zero wind speed case where the rotor is still and the 11.4 m/s case

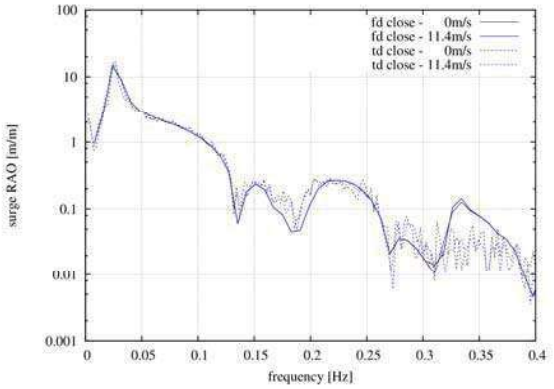

Figure 4: Surge RAO's comparison

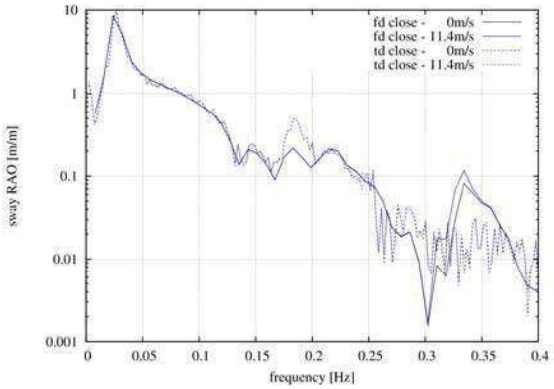

Figure 5: Sway RAO's comparison

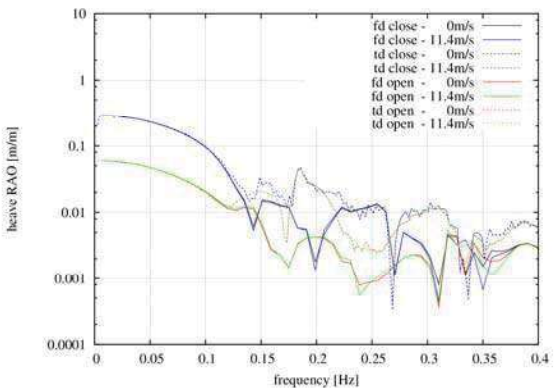

Figure 6: Sway RAO's comparison

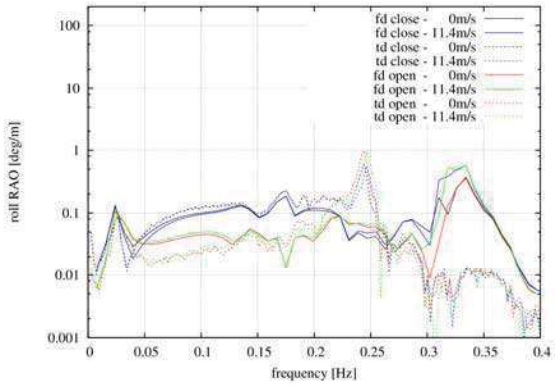

Figure 7: Roll RAO's comparison

which corresponds to the rated wind speed at which the rotational speed is 12 rpm. The wave heading angle is 30 deg.

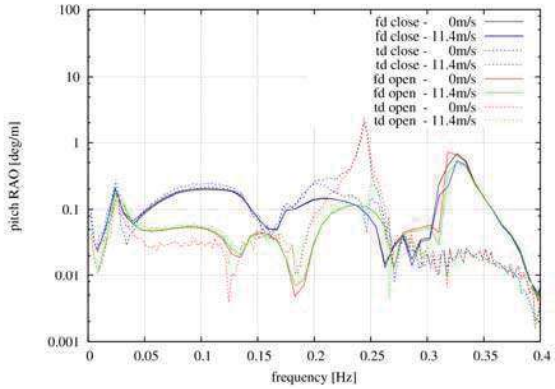

Figure 8: Pitch RAO's comparison

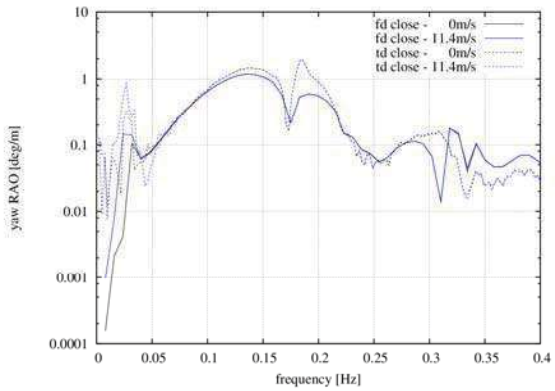

Figure 9: Yaw RAO's comparison

The 'open' case RAOs plots in the heave, roll and pitch motions correspond to the case where the OWC does not contribute additional pressure terms. The surge, sway and yaw RAO's are not affected by the OWC. Time domain simulations consider additional elastic degrees of freedom and nonlinear modeling of the aerodynamics, the complete dynamics, the mooring lines and the viscous term of the Morison's equation. Both methods consider the same linear hydrodynamic theory.

In general both methods predict similar RAOs and the eigen frequencies of table 1 are clearly identified. Focusing on the differences, in the frequency domain results the surge-pitch and the sway-roll coupling at 0.35 Hz are excited, contrary to that shown in the time domain ones (Figures 4, 5). Excellent agreement is observed in the heave motion (Figure 6) up to 0.15 Hz. At higher frequencies the heave exciting force, which is not presented due to space limitation, is almost zero and explains the difference. In the roll and the pitch motions (Figures 7, 8) the reduction of the natural frequency is clearly depicted, as already discussed in section 4.1. Both methods capture the reduction of the roll and pitch amplitudes at the corresponding eigen frequencies due to the aerodynamic damping. The influence of the aerodynamic damping in the time domain predictions is by far more significant due to nonlinear aerodynamics. It is noted that viscous drag could not be the reason, because it is present in the 0 wind case as well, in which the amplitudes are high and comparable to those in the frequency domain results. The OWC also does not seem to influence the peak amplitude, as the roll and pitch eigen frequencies are outside the wave region. In the range of the wave frequencies, the amplitudes of the heave (Figure 6) and the roll/pitch (Figures 7, 8) motions are more excited when the contribution of the OWC is considered. Finally, the time domain method predicts slightly higher yaw amplitude RAOs. Both methods capture the gyroscopic effects at

~0.03 Hz where the rotation of the blade increases the yaw motion.

5. CONCLUSIONS

A TLP floater supporting the NREL 5MW RWT and 3 OWC devices has been analyzed. For this design, RAO's of the complete system have been calculated using frequency as well as time domain simulations.

By comparing the results from the two methods, the following conclusions were drawn:

1 Both methods consistently predict the system RAO's, which gives confidence to the specific frequency domain approach as a preliminary design tool.

2 The frequency domain method does not include structural flexibilities which affect the roll/pitch RAO's. The natural frequency in roll/pitch for the rigid WT is 0.3Hz, while for the flexible WT is 0.25Hz and the tower bending frequencies about 0.85Hz. On the other hand roll and pitch is very small for a TLP - in time domain calculations do not exceed 0.1 deg. - and not within the wave frequency range.

3 As regards the design, it seems difficult to increase the roll/pitch natural frequencies above 0.25 Hz and keep the cost reasonable, due to the strong coupling with the tower that is counteracting.

4 Both methods capture the aerodynamic damping that reduces the amplitude of the roll/pitch motions around resonance and the gyroscope effect affecting the yaw amplitude.

5 The roll and pitch RAO's amplitudes near resonance as predicted by the time domain method are smaller, most probably due to aerodynamic nonlinearities, and not viscous damping as was initially supposed.

6 The action of the OWC devices increase heave, roll and pitch RAO's. In this respect, the IEC load cases should be performed in time domain.

6. ACKNOWLEDMENTS

This research has been co-financed by the European Union (European Social Fund – ESF) and Greek national funds through the Operational Program "Education and Lifelong Learning" of the National Strategic Reference Framework (NSRF) 2007 – 2013: Research Funding Program: ARISTEIA, Program POSEIDON (2041).

7. REFERENCES

Aubault, A., Alves, M., Sarmento, A., Roddier, D., Peiffer, A., 2011. Modeling of an oscillating water column on the floating foundation WINDFLOAT; Proceedings, 30th International Conference on Ocean, Offshore and Arctic Engineering (OMAE2011), Rotterdam, The Netherlands.

Evans, D.V., Porter, R., 1996. Efficient calculation of hydrodynamic properties of OWC type devices; OMAE–Volume I – Part B; p. 123–132.

Falnes, J., 2002. Ocean waves and oscillating systems: linear interactions including wave-energy extraction; Cambridge University Press.

Jonkman, J., Butterfield, S., Musial, W. and Scott G., 2009 Definition of a 5-MW Reference Wind Turbine for Offshore System Development, Technical Report, NREL/TP-500-38060, USA.

Konispoliatis, D.N., Mavrakos, S.A., 2013 a. Hydrodynamics of multiple vertical axisymmetric OWC's devices restrained in waves; Proceedings, 32nd International

Conference Ocean, Offshore and Arctic Engineering (OMAE2013), Nantes, France.

Konispoliatis, D.N., Mavrakos, S.A., 2013 b. Hydrodynamics of arrays of OWC's devices consisting of concentric cylinders restrained in waves; Proceedings, 10th European Wave and Tidal Energy Conference (EWTEC 2013), International Conference Ocean, Aalborg, Denmark.

Manolas, D., Riziotis, V., Voutsinas, S., 2012. Assessment of 3D aerodynamic effects on the behaviour of floating wind turbines, The science of making torque from Wind, TORQUE 2012, Oldenbourg, Germany.

Martins–rivas H. & Mei C.C., 2009. Wave power extraction from an oscillating water column along a straight coast. In: Ocean Engineering 36; p. 426–433.

Mavrakos, S.A. & Koumoutsakos, P., 1987. Hydrodynamic interaction among vertical axisymmetric bodies restrained in waves; Applied Ocean Research, Vol. 9, No. 3.

Mavrakos, S.A., 1991. Hydrodynamic coefficients for groups of interacting vertical axisymmetric bodies; Ocean Engineering, Vol. 18, No. 5, p. 485–515.

Mavrakos, S.A., Chatjigeorgiou, I.K., Mazarakos, T., Konispoliatis, D.N, Maron, A., 2011. Hydrodynamic forces and wave run-up on concentric vertical cylinders forming piston-like arrangements; Proceedings, 26th International Workshop on Water Waves and Floating Bodies, Athens, Greece.

Mazarakos, T.P., Mavrakos, S.A., Konispoliatis, D.N., Voutsinas, S.G., Manolas, D., 2014a. Multi- purpose floating structures for offshore wind and wave energy sources exploitation. COCONET Workshop for Offshore Wind Farms in the Mediterranean and Black Seas, Anavyssos- Greece, *9- 10 June 2014*.

Mazarakos, T.P., Manolas, D.I., Grapsas T., Mavrakos, S.A., Riziotis V.A., Voutsinas S.G., 2014b, Conceptual design and advanced hydro-aero-elastic modeling of a TLP concept for floating wind turbine applications. RENEW 2014, *Lisbon, Portugal*.

Newman, J.N., 1977. The motions of a floating slender torus; J. Fluid Mech, Vol. 83, p. 721–735.

Okhusu, M., 1974. Hydrodynamic forceson multiple cylinders in waves; Int. Symp. on the Dynamics of Marine Vehicles and structures in Waves, University College London, London.

Papadakis, G., Riziotis, V., Voutsinas, S., Mavrakos, S.A., 2014. W/T's reduced order aeroelastic models (in Greek). Technical Report No. D3.2, Program POSEIDON (2014), Greek General Secretariat for Research and Technology.

Popko et al., 2012. Offshore Code Comparison Collaboration Continuation (OC4), Phase I – Results of Coupled Simulations of an Offshore Wind Turbine with Jacket Support Structure, ISOPE 2012, Rhodes, Greece.

Riziotis. V.A., Voutsinas, S.G., 1997. GAST: A general aerodynamic and structural prediction tool for wind turbines. Procerdings of the EWEC' 97, Dublín, Ireland, 1997.

Riziotis, V., S.G. Voutsinas, E.S. Politis, P.K. Chaviaropoulos 2004. Aeroelastic Stability of Wind Turbines: the problem, the methods, the issues", Wind Energy, 7, pp 373-392.

Robertson Amy et al., 2014. Offshore code comparison collaboration, continuation within IEA wind task 30: phase II results regarding a floating semisubmersible wind system, OMAE 2014, San Francisco, USA.

Twersky, V., 1952. Multiple scattering of radiation by an arbitrary configuration of parallel cylinders; J. Acoustical Soc. of America, 24 (1).